

Branimir N. Grgur\*

Faculty of Technology and Metallurgy University of Belgrade,  
Belgrade, Serbia

Scientific paper

ISSN 0351-9465, E-ISSN 2466-2585

UDC:691.714.018.8:669.295:54-145.15

doi: 10.5937/zasmat2004339G



Zastita Materijala 61 (4)  
339 - 345 (2020)

## Corrosion of the stainless steel 316Ti in 10% hydrochloric and sulfuric acid

### ABSTRACT

*The corrosion of the austenitic stainless steel 316Ti is investigated in 10% hydrochloric and 10% sulfuric acid, by the means of linear polarization, electrochemical impedance spectroscopy, polarization, and weight loss measurements. It is concluded that 316Ti is unstable in 10% hydrochloric acid and passive in 10% sulfuric acid solution.*

**Keywords:** Austenitic stainless steel; Titanium; Weight loss; Micrographs.

### 1. INTRODUCTION

The austenitic stainless steel (SS) 316Ti due to the addition of the titanium has improved mechanical characteristics and improved corrosion resistance in comparisons with similar stainless steels SS 316 and SS 316L grade containing molybdenum. The titanium atoms stabilize the structure of the stainless steel at elevated temperatures above 800°C, avoiding the carbide precipitation at the grain boundaries and protects the metal from corrosion. SS 316Ti is also known as X6CrNiMoTi17-12-2; AISI/SAE 316Ti; UNS S31635 or EN 1.4571 [1]. The SS 316Ti has a broad range of uses, like equipment for the food processing, brewery, vine, chemical and petrochemical equipment, laboratory benches and equipment, seaside architectural paneling and balustrading, boat fittings, chemical transportation containers, heat exchangers, medical implants, etc. [1].

The corrosion behavior of SS 316Ti is less studied than SS 316, 316L, and 304 [2-10]. The corrosion behavior of SS 304, 316, and 316Ti in aqueous solutions of methanesulfonic acid is investigated by Finšgar and Milošev [11].

They find comparable corrosion behavior for all three grades. Loto [12] investigated the corrosion resistance of austenitic 316Ti, martensitic GX4CrNiMo16-5-1 (EN 1.4405), and ferritic 444 stainless steel in 1 M sulfuric acid solution with the addition of 0%-6% NaCl. He found that 316Ti is less resistant to the acidic solution in the presence of the chloride ions. Lorschach and Schmitz [13] showed that agitation rate has important influence in the increases of the corrosion rate of SS 316Ti in an acidic (250 ppm Cl<sup>-</sup>, pH = 4, *t* = 30°C) and an alkaline (4% Cl<sup>-</sup>, pH = 9, *t* = 80°C) electrolytes. Pardo et al. [14] investigated the influence of Ti, C, and N concentration in SS 316Ti and SS 321 on the intergranular corrosion after different heat treatments in the solution of 0.5 M H<sub>2</sub>SO<sub>4</sub> + 0.01 M KSCN at 30°C. They determined that the addition of titanium promotes improved intergranular corrosion resistance of the stainless steel due to the precipitation of TiC, which reduces the formation of chromium-rich carbides. Besides, they concluded that SS 316Ti retains better intergranular corrosion resistance than SS 321. Zhao et al. [15] investigated stabilizing treatment on microstructure and intergranular corrosion resistance of 316Ti stainless steel in 0.5M H<sub>2</sub>SO<sub>4</sub> + 0.01M KSCN at 25°C and showed that intergranular corrosion resistance increased with increasing aging temperature.

The corrosion of SS 316Ti is sporadically reported; consequently, the aim of this work is to investigate the corrosion resistivity of SS 316Ti in

\*Corresponding author: Branimir N. Grgur

E-mail: BNGrgur@tmf.bg.ac.rs

Paper received: 05. 10. 2020.

Paper accepted: 22. 10. 2020.

Paper is available on the website:  
www.idk.org.rs/journal

10% of sulfuric and 10% hydrochloric acid, using different electrochemical techniques and weight loss measurements.

## 2. EXPERIMENTAL

The SS 316Ti, with nominal (N.C.) and chemical (C.C) composition is given in table 1.

Table 1. Nominal (N.C) and chemical (C.C) composition of SS 316Ti

Tabela 1. Nominalni (N.C) i hemijski (C.C) sastav SS 316Ti

Element	C	Si	P	S	Cr	Ni	Mo	Mn	Ti*	Fe
N.C, wt%	≤0.08	≤1.0	≤0.045	≤0.015	16.5–18.5	10.5–13.5	2.0–2.5	0–2	≤0.70	balance
C.C, wt%	0.04	0.42	0.025	0.002	16.7	10.6	2.12	1.3	0.42	balance

\*The minimum Ti content should be 5×C wt%.

As a corrosion media, 10% of sulfuric and hydrochloric acid, prepared by dilution of concentrated acids (p.a. Merck) in distilled water is used.

The electrochemical measurements are performed in a three-compartment glass cell with a volume of 100 cm<sup>3</sup> open to the air. As a working electrode, the sample with dimensions 3×3×30 mm, with exposed surface area to the electrolyte of  $S = 2.23 \text{ cm}^2$ , is used. Specimens are wet ground to 1200 grit SiC paper, followed by ultrasonic washing in isopropanol. Platinum foil and saturated calomel electrodes are used as counter and reference electrodes, respectively. Electrochemical measurements are conducted using potentiostat-galvanostat Gamry 1010E. Simultaneously with corrosion potential measurements during 55 minutes (ASTM Designation: G 59–97) polarization resistance,  $R_p$ , is determined using  $R_p/E_{\text{corr}}$ -trend ( $\pm 10 \text{ mV}$  vs  $E_{\text{corr}}$ ) software. Electrochemical impedance measurements are performed in a frequency range of 50 kHz to 10 mHz with AC amplitude of  $\pm 10 \text{ mV}$  at corrosion potential. For the

polarization measurements potentiodynamic,  $v = 1 \text{ mV s}^{-1}$ , techniques is used.

Weight loss measurement is conducted in 200 cm<sup>3</sup> of 10% aerated solutions of the acids using the sample with dimensions of 24×25×3 mm with the surface area of 16.7 cm<sup>2</sup>, for 77 h at 25°C. After the weight loss measurement, an optical microscope Olympus CX41 equipped with a digital camera and connected to the PC is used to analyze the samples.

## 3. RESULTS AND DISCUSSION

Figure 1 shows the dependence of the open-circuit potentials of SS 316Ti during 55min of immersion in 10% acids. For the sample immersed in 10% sulfuric acid, after the initial decrease, for 10 min. potential has stabilized at  $-0.235 \text{ V}$ . For the sample in 10% hydrochloric acid, a slight increase of the potential is observed, and after 55 min. reaches a value of  $-0.35 \text{ V}$ . Therefore, for both cases, the main cathodic reaction is hydrogen evolution reaction.

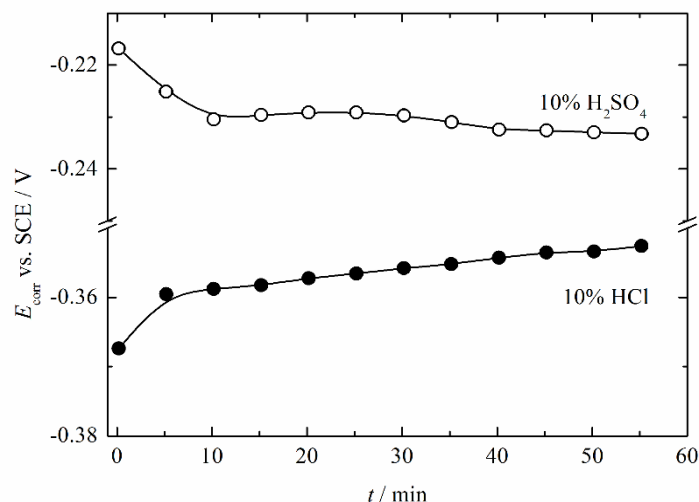


Figure 1. The dependence of the corrosion potentials of the samples immersed in 10% hydrochloric and 10% sulfuric acid

Slika 1. Zavisnost potencijala korozije uzoraka uronjenih u 10% hlorovodoničnu i 10% sumpornu kiselinu

The polarization resistance of the sample in 10% sulfuric acid, Fig.2, during immersions, constantly increases from  $\sim 200 \Omega \text{cm}^2$  to  $3730 \Omega \text{cm}^2$ . This indicates the growth of the passive film onto

the electrode surface. On the contrary, the sample immersed in 10% hydrochloric acid constantly decreased from  $\sim 250 \Omega \text{cm}^2$  to  $\sim 165 \Omega \text{cm}^2$ , indicating passive film breakdown.

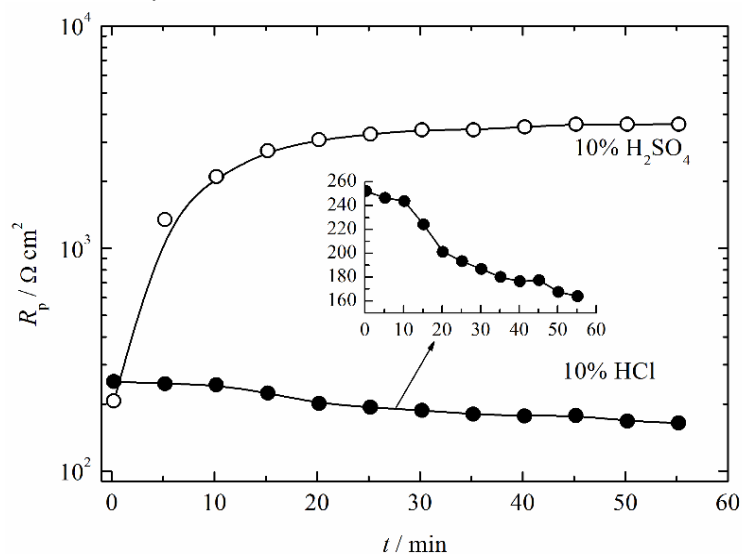


Figure 2. The dependence of the polarization resistance of the samples immersed in 10% hydrochloric and 10% sulfuric acid

Slika 2. Zavisnost polarizacionog otpora uzoraka uronjenih u 10% hlorovodoničnu i 10% sumpornu kiselinu

Immediately after recording corrosion potentials, the electrochemical impedance spectra are taken. From Fig. 3 can be seen that overall impedance is for an order of magnitude higher in 10% sulfuric than in 10% hydrochloric acid. In sulfuric acid, one depressed semicircle is

observed. In 10% hydrochloric acid one slightly depressed semicircle and inductive loop at low frequencies are observed. The inductive loop is probably induced by strong adsorption of chloride ions from solution onto the electrode surface [16].

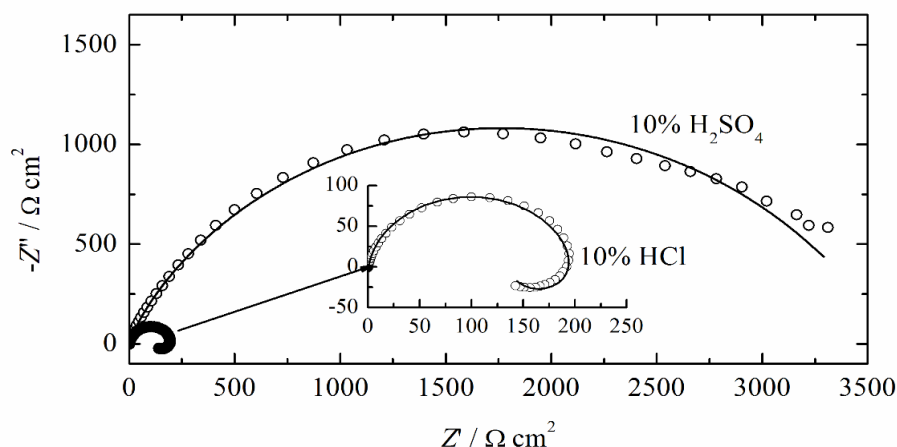


Figure 3. The electrochemical impedance spectra of the 316Ti in 10% hydrochloric and 10% of sulfuric acids. Open circles-experimental points, line-best fit

Slika 3. Spektri elektrohemijske impedanse 316Ti u 10% hlorovodoničnoj i 10% sumporne kiseline. Otvoreni krugovi - eksperimentalne tačke, linije-najbolji fit

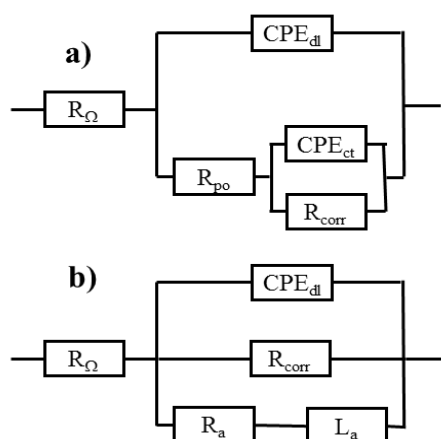


Figure 4. The equivalent electrical circuit for the impedance fitting in a) 10%  $\text{H}_2\text{SO}_4$  and b) 10%  $\text{HCl}$

Slika 4. Ekvivalentna električna kola za fitovanje impedanse u a) 10%  $\text{H}_2\text{SO}_4$  i b) 10%  $\text{HCl}$

Used equivalent electrical circuits are shown in Fig. 4.  $R_\Omega$  represent the Ohmic drop in the solution.

Double-layer capacitance is represented with constant phase elements ( $\text{CPE}_{\text{dl}}$ ). The deviation from a purely capacitive behavior might be explained by 2D heterogeneities. The  $\text{CPE}_{\text{ct}}$  is assigned to the capacitance of adsorbed intermediates during the corrosion processes. The impedance of CPE is given as:

$$Z = \frac{1}{Y_0(j\omega)^n} \quad (1)$$

and for  $n = 1$   $Y_0 = C$ .  $R_{\text{po}}$  is assigned to the pore resistance of the passive film, while  $R_{\text{corr}}$  corresponds to the corrosion processes.  $R_a$  and  $L_a$  are resistance and inductivity of the process of the chloride adsorption [17]. From Fig.4, it can be seen that fitted lines well corresponds to the experimental points. Table 2 summarizes the obtained parameters of the impedance fitting.

Table 2. Obtained parameters of the corrosion process determined from the impedance measurements

Tabela 2. Dobijeni parametri procesa korozije utvrđeni na osnovu merenja impedanse

	$R_\Omega$ $\Omega \text{ cm}^2$	$Y_{0,\text{dl}}$ $\text{S s}^n$	$n$	$R_{\text{po,(a)}}$ $\Omega \text{ cm}^2$	$Y_{0,\text{ct}}$ $\text{S s}^n$	$n$	$R_{\text{corr}}$ $\Omega \text{ cm}^2$	$L$ $\text{k}\Omega \text{ s cm}^2$
10% $\text{H}_2\text{SO}_4$	0.94	$2.43 \times 10^{-4}$	0.65	0.007	$27 \times 10^{-6}$	1.0	3625	
10% $\text{HCl}$	0.49	$5.7 \times 10^{-4}$	0.92	439	-	-	185	3.43

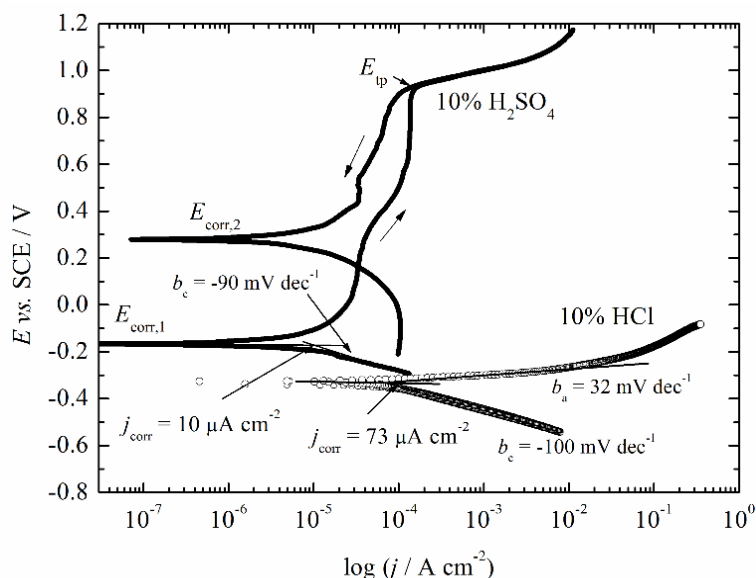


Figure 5. Polarization curves in 10% hydrochloric and 10% sulfuric acid

Slika 5. Polarizacione krive u 10% hlorovodoničnoj i 10% sumpornoj kiselini

Figure 5. shows the polarization curves of SS316Ti. In 10% hydrochloric acid, the active anodic dissolution is observed up to the current density of  $400 \text{ mA cm}^{-2}$ , characterized by the Tafel slope of  $32 \text{ mV dec}^{-1}$ . The cathodic polarization curve with the Tafel slope of  $-100 \text{ mV dec}^{-1}$ , corresponds to the hydrogen evolution reaction. From the intercept of anodic and cathodic Tafel lines with corrosion potential, the corrosion current density of  $73 \text{ } \mu\text{A cm}^{-2}$  is determined. In sulfuric acid solution, from the cathodic Tafel slope of  $-90 \text{ mV dec}^{-1}$ , the corrosion current density of  $\sim 10 \text{ } \mu\text{A cm}^{-2}$  is determined from the intercept with  $E_{\text{corr},1}$ . After  $E_{\text{corr},1}$  the passivation of the steel occurred without the active dissolution region. The passive region from  $0 \text{ V}$  to  $\sim 0.94 \text{ V}$  is characterized by two regions of passivity. The first one from  $0 \text{ V}$  to  $0.35 \text{ V}$  with passive current density between  $30$  to  $40 \text{ } \mu\text{A cm}^{-2}$ , and the second one from  $0.35 \text{ V}$  to  $\sim 0.93 \text{ V}$  with passive current density between  $130$  to  $140 \text{ } \mu\text{A cm}^{-2}$ . After  $0.94 \text{ V}$ , transpassive region is observed. In the reverse scan, repassivation of the steel coincidence with transpassive potential, and passive state is stable up to the  $E_{\text{corr},2}$ , at  $0.29 \text{ V}$ , followed by the cathodic reaction of the oxygen reduction reaction. Because,  $E_{\text{corr},2}$  is higher than  $E_{\text{corr},1}$  the tendency to pitting corrosion could not be expected.

In order to compare linear polarization data, EIS and polarization data, the corrosion current density is determined using equation:

for hydrochloric acid

$$j_{\text{corr}} = \frac{b_a |b_c|}{2.3 R_p (b_a + |b_c|)} \quad (2)$$

where  $b_{a,c}$  are estimated anodic and cathodic Tafel slopes  $0.032 \text{ Vdec}^{-1}$ , and  $-0.1 \text{ Vdec}^{-1}$  Fig. 5, and for the sulfuric acid, for  $b_c = -0.090 \text{ Vdec}^{-1}$ :

$$j_{\text{corr}} = \frac{|b_c|}{2.3 R_p} \quad (3)$$

because  $b_a \rightarrow \infty$ .

In Table 3 the summarized corrosion parameters obtained from the polarization, linear polarization, and impedance measurements are shown. For the sulfuric acid with all three methods practically the same corrosion current density of  $\sim 10.4 \text{ } \mu\text{A cm}^{-2}$  is obtained. For the hydrochloric acid, due to the very fast reaction, some dissipation of the values of corrosion current density is obtained. The middle value is  $65 \pm 8 \text{ } \mu\text{A cm}^{-2}$ .

Table 3. Corrosion parameters obtained by applying polarization (pol), linear polarization (lp), and electrochemical impedance spectroscopy (imp)

Tabla 3. Korozioni parametri dobijeni primenom polarizacije (pol), linearne polarizacije (lp) i elektrohemijske impedansne spektroskopije (imp)

	$E_{\text{corr}}$ V	$j_{\text{corr(pol)}}$ $\mu\text{A cm}^{-2}$	$R_p(\text{lp})$ $\Omega \text{ cm}^2$	$j_{\text{corr(lp)}}$ $\mu\text{A cm}^{-2}$	$R_p(\text{imp})$ $\Omega \text{ cm}^2$	$j_{\text{corr(imp)}}$ $\mu\text{A cm}^{-2}$	K $\text{mm yr}^{-1}$
10% $\text{H}_2\text{SO}_4$	-0.166	10	3730	10.5	3625	10.8	0.115
10% HCl	-0.334	73	165	64	185	57	$0.72 \pm 0.09$

From the determined corrosion current densities, the corrosion rate can be estimated using the following equation:

$$K(\text{mm/year}) = \frac{\Delta m}{\rho(\text{SS})} = \frac{10 \times j_{\text{corr}} \times t \times M(\text{SS})}{\rho(\text{SS}) \times n \times F} \quad (4)$$

where  $\rho(\text{SS}) = 7.82 \text{ g cm}^{-3}$  is the alloy density,  $t = 8760$  hours in a year, 10 is a conversion factor from cm in mm,  $M(\text{SS}) = 55.63 \text{ g mol}^{-1}$  molar mass of the alloy,  $n = 2.1$  is an average number of exchanged electrons and  $F = 26.8 \text{ Ah mol}^{-1}$  Faraday constant. According to standard ASTM Designation: G102 – 89:  $\rho(\text{SS})$ ,  $M(\text{SS})$  and  $n$  are calculated according to:

$$M(\text{SS}) = \sum M(M_i) \times x_i$$

$$\rho(\text{SS}) = \sum \rho(M_i) \times x_i$$

$$n(\text{SS}) = \sum n(M_i) \times x_i$$

where index  $i$  corresponds to single metal (M) components in the alloy, and  $x$  to the mass fraction of the metal in the stainless steel. From table 3, can be seen that the corrosion rate,  $K$ , is almost seven times faster in hydrochloric than in sulfuric acid.

The corrosion rate by weight loss is determined by exposing specimens with dimensions of  $24 \times 25 \times 3 \text{ mm}$  with an area of  $16.7 \text{ cm}^2$  to  $200 \text{ cm}^3$  of 10% of aerated acids at a temperature of  $25^\circ\text{C}$

for 77 h. The corrosion rate is calculated based on the change in mass before and after the exposure to acidic media. After completion of the corrosion test, the sample is washed with distilled water, dried in a stream of warm air, and weighed on an analytical balance with an accuracy of  $\pm 0,0001$  g. The measured change in the alloy mass after the corrosion test for 77 hours (3.21 days) at 25°C are in hydrochloric acid  $\Delta m = m_1 - m_2 = 13.7068 - 13.5822 = 0.1246$  g, and for sulfuric acid,  $\Delta m = m_1 - m_2 = 13.8321 - 13.8195 = 0.0126$  g.

Based on the change in mass, the corrosion rate,  $K$  is determined using the equation:

$$K = \frac{10 \times \Delta m \times 365 \text{ days}}{S \times \rho \times 3.21 \text{ days}} \quad (5)$$

where  $\rho = 7,8 \text{ g cm}^{-3}$ , is the alloy density,  $S = 16,7 \text{ cm}^2$  surface area of the sample,  $\Delta m$  mass change in g, and 10 conversion factor of cm in mm. For the hydrochloric acid,  $K = 1.088 \text{ mm yr}^{-1}$ , which is higher than values obtained by electrochemical techniques, indicating that during the time corrosion is accelerated, probably due to increases of the real surface of the specimens. For the sulfuric acid corrosion rate,  $K = 0.11 \text{ mm yr}^{-1}$ , is consistent with the electrochemical measurements.

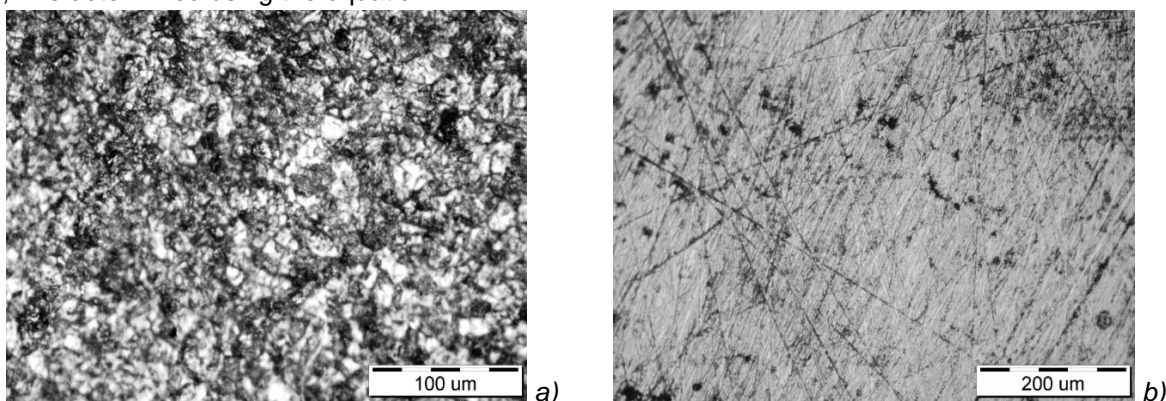


Figure 6. Optical micrographs of a sample a) exposed to 10% hydrochloric acid, and b) to 10% sulfuric acid, during 77 h

Slika 6. Optička mikrofotografija uzorka a) izložena 10% hlorovodoničnoj kiselinu i b) 10% sumpornoj kiselinu, tokom 77 h

The optical micrograph of the stainless steel surface after exposure to 10% hydrochloric acid, Fig 6a, showed a highly corroded and damaged area along with visible grains, indicating intergranular corrosion, which is attributed due to acid attack of metal. The surface exposed to 10% of sulfuric acid, Fig 6b, remains practically unaffected, indicating slow homogeneous corrosion without pitting or any other types of heterogeneous corrosion.

#### 4. CONCLUSIONS

The corrosion of stainless steel 316Ti is investigated in 10% hydrochloric and 10% of sulfuric acid. Using the different electrochemical techniques the average corrosion current density of  $65 \pm 8 \mu\text{A cm}^{-2}$  and corrosion rate of  $0.72 \pm 0.09 \text{ mm yr}^{-1}$  for 10% hydrochloric acid, and  $\sim 10.4 \mu\text{A cm}^{-2}$  with corrosion rate of  $0.115 \text{ mm yr}^{-1}$  for 10% sulfuric acid is determined. By the weight loss measurements, for the 10% hydrochloric acid,  $K = 1.088 \text{ mm yr}^{-1}$  is determined, indicating that during the time corrosion is accelerated, probably due to increases of the real surface of the specimens. For

the 10% sulfuric acid corrosion rate,  $K = 0.11 \text{ mm yr}^{-1}$ , is consistent with the electrochemical measurements.

#### Acknowledgment

This work is supported by the Ministry of Education, Science and Technological Development of the Republic of Serbia (Contract No. 451-03-68/2020-14/200135)

#### 5. REFERENCES

- [1] Aalco Metals Ltd, UK, [http://www-eng.lbl.gov/~shuman/NEXT/MATERIALS&COMPONENTS/Pressure\\_vessels/Aalco-Metals-Ltd\\_Stainless-Steel\\_1.4571-316Ti\\_40.pdf](http://www-eng.lbl.gov/~shuman/NEXT/MATERIALS&COMPONENTS/Pressure_vessels/Aalco-Metals-Ltd_Stainless-Steel_1.4571-316Ti_40.pdf) (Accessed 1 October 2020.)
- [2] W.Y.Lai, W.Z.Zhao, Z.F.Yin, J.Zhang (2012) Electrochemical and XPS studies on corrosion behaviours of AISI 304 and AISI 316 stainless steels under plastic deformation in sulphuric acid solution, *Surf. Interface Anal.*, 44, 505-512.
- [3] M.Zakeri, M.Naghizadeh, D.Nakhaie, M.H.Moayed (2016) Pit transition potential and repassivation potential of stainless steel in thiosulfate solution, *J. Electrochem. Soc.*, 163(6), C275-C281.

- [4] P.Dhaiveegan, N.Elangovan, T.Nishimura, N. Rajendran (2016) Corrosion behavior of 316L and 304 stainless steels exposed to industrial-marine-urban environment: field study, RSC Adv., 6, 47314-37324.
- [5] E.Otero, A.Pardo, M.V.Utrilla, F.J.Pérez, C.Merino (1997) The corrosion behaviour of AISI 304L and 316L stainless steels prepared by powder metallurgy in the presence of organic acids, Corros. Sci., 39, 453-463.
- [6] R.T.Loto (2017) Study of the corrosion resistance of type 304L and 316 austenitic stainless steels in acid chloride solution. Orient J Chem., 33(3), 1090-1096.
- [7] G.H.Aydoğdu, M.K.Aydinol (2006) Determination of susceptibility to intergranular corrosion and electrochemical reactivation behaviour of AISI 316L type stainless steel, Corros. Sci., 48, 3565-3583.
- [8] Y.Yi, P.Cho, A. Al Zaabi, Y.Addad, C.Jang (2013) Potentiodynamic polarization behaviour of AISI type 316 stainless steel in NaCl solution, Corros. Sci., 74, 92-97.
- [9] Z.Duana, C.Mana, C.Dong, Z.Cui, D.Kong, L. Wang, X.Wang (2020) Pitting behavior of SLM 316L stainless steel exposed to chloride environments with different aggressiveness: Pitting mechanism induced by gas pores, Corros. Sci., 167, article 108520.
- [10] B.Malinović, T.Djuričić, D.Zorić (2020) Corrosion behaviour of stainless steel EN 1.4301 in acid media in presence of PBTCA inhibitor, Zastita Materijala, 61(2), 133-139.
- [11] M.Finšgar, I.Milošev (2010) Corrosion behaviour of stainless steels in aqueous solutions of methanesulfonic acid, Corros. Sci., 52, 2430-2438.
- [12] R.T.Loto (2019) Corrosion resistance and morphological deterioration of 316Ti austenitic, GX4CrNiMo16-5-1 martensitic and 444 ferritic stainless steels in aqueous corrosive environments, Results Phys., 14, article 102423.
- [13] B.Lorsbach, E.Schmitz (2018) Influence of test parameters of potentiodynamic current density measurements on the determination of the pitting corrosion resistance of austenitic stainless steels. Mat. Corr., 69, 37-43.
- [14] A.Pardo, M.C.Merino, A.E.Coy, F.Viejo, M. Carboneras, R.Arrabal (2007) Influence of Ti, C and N concentration on the intergranular corrosion behaviour of AISI 316Ti and 321 stainless steels, Acta Mater., 55, 2239-2251.
- [15] B.Zhao, W.Zhao, H.Shi, G.Li, Y.Ding (2019) The effects of stabilizing treatment on microstructure and corrosion resistance of 316Ti stainless steel, Eng. Fail. Anal., 105, 961-969.
- [16] L.Bai, B.E.Conway (1991) AC impedance of faradaic reactions involving electroadsorbed intermediates. Examination of conditions leading to pseudoinductive behavior represented in three-dimensional impedance spectroscopy diagrams, J. Electrochem. Soc., 138, 2897-2907.
- [17] A.Singh, Y.Caihong, Y.Yaocheng, N.Soni, Y.Wu, Y. Lin (2019) Analyses of new electrochemical techniques to study the behavior of some corrosion mitigating polymers on N80 tubing steel, ACS Omega, 4, 3420-3431.

## IZVOD

### KOROZIJA NERĐAJUĆEG ČELIKA 316Ti U 10% HLOROVODONIČNOJ I SUMPORNOJ KISELINI

*Korozija austenitnog nerđajućeg čelika 316Ti ispitivana je u 10% hlorovodoničnoj i 10% sumporne kiseline, pomoću linearne polarizacije, elektrohemijske impedanse spektroskopije, polarizacionih merenja i merenja gubitka težine. Zaključeno je da je 316Ti nestabilan u 10% hlorovodoničnoj kiselini i pasivan u rastvoru 10% sumporne kiseline.*

**Ključne reči:** Austenitni nerđajući čelik, titan, gubitak mase, mikrografija.

*Naučni rad*

*Rad primljen: 05. 10. 2020.*

*Rad prihvaćen: 22. 10. 2020.*

*Rad je dostupan na sajtu: [www.idk.org.rs/casopis](http://www.idk.org.rs/casopis)*